JOURNAL OF MECHANICAL ENGINEERING AND SCIENCES
ISSN: 2289-4659 e-ISSN: 2231-8380
VOLUME 17, ISSUE 3, 2023, 9616 – 9628
DOI: https://doi.org/10.15282/jmes.17.3.2023.7.0761

RESEARCH ARTICLE

Experimental investigation on the effect of process variables for the quality characteristics of AA 2024 processed in cold extrusion

K. A. Francy[1]*, C. S. Rao[2]

[1] Vishnu Institute of Technology, Bhimavaram, West Godavari, Andhra Pradesh, 534202, India
[2] Andhra University College of Engineering, Visakhapatnam, Andhra Pradesh, 530003, India

ABSTRACT - Extrusion process has many applications in manufacturing industries due to its ability to produce products of high quality. Extrusion process can be classified into hot extrusion and cold extrusion. The cold forward extrusion is carried out at ambient temperature and has the additional benefit of improved mechanical characteristics. The metarial is compressed under intense pressure through a die orifice with a specific shape during the extrusion process. This process is effected by a few process variables, including die angle, punch speed, and lubrication are in greater extent towards the extrusion force requirement, microstructure and the product quality. Hence, the present experimental work focuses on extrusion of circular billet to produce cylindrical rod. Studying the behaviour of the material and the importance of the input process parameters during the cold extrusion process is the primary goal of this work. The experiments are carried out with AA 2024 alloy because of its wide applications in navy and aircraft structures. The varying die angles (10°, 20° & 30°) as well as punch speed (1.6 mm/min, 3.2 mm/min and 4.8 mm/min) and lubricants (molybdium sulphide (MoS_2), zinc stearate and grease) chosen as input parameters. The out put responses of this extrusion process are extrusion force, displacement, time and surface roughness. Extrusion forces are calculated based on flow stress curves at the locations of greatest elastic deformation. The results shows that increasing the punch speed and die angle increases the extrusion force. The microstructure evolutions and grain refinement at different die angles are examined using electron back scatter diffraction analysis. At 30° die angle, the microstructure showed grain refinement. It is also noted that the damage is significant at 30° die angle with a punch speed above 4.8 mm/min.

ARTICLE HISTORY

Received	:	01st Jan. 2023
Revised	:	15th July 2023
Accepted	:	04th Aug. 2023
Published	:	28th Sept. 2023

KEYWORDS

Die angle
Extrusion force
Microstructure
Misorientation
Punch speed

1.0 INTRODUCTION

Aluminium have been designed as “the new millennium's metal" in recent years [1]. Extruded aluminium is extensively used in aerospace, construction and automotive industries [2]. Extrusion is a process that uses a hydraulic press to force a round billet through a die in order to shape it into the desired shape. The induced shear and compression forces lead the stress to build until it reaches the plastic flow occurs through the die. Cold and hot extrusion are two different types of extrusion processes. Compared to hot extrusion, cold extrusion has the added benefit of better mechanical properties [3]. The main advantage of cold extrusion includes close tolerance, lack of oxidation, good surface finish.

The literature contains a number of experimental and numerical studies to understand how the process parameters affect the extrusion process. Adeosun et al. [4] performed the experimental work on the impact of different die angles on the extrusion behaviour of wrought aluminium alloy with various die angles are from 15° to 90°. Among all the dies the highest extrusion pressure achieved for 30° die angle. It was concluded that similar behaviour available at some more die angles are 15°, 30° and 45° when the ram displacement of 1 to 13 mm. In order to understand the die failure modes due to the complexity of the extruded profile, extrusion pressure and material flow are analysed during the aluminium extrusion process [5]. Extrusion pressure and stress variations are examined in a porthole die of extrusion thin-walled profiles [6]. Aluminium product defects are described and assessed [7]. Onuh et al. [8] conducted both experimental work and Finite Element Analysis simulation. The investigation was performed to estimate impact of die angle, reduction ratio, and extrusion force in extrusion process. Both the radius of curvature for extruded alloys of lead and aluminium as well as the average hardness value of the extruded products along projections and circumferential solid places are observed. Hardness increases slightly with increasing load rates and slightly with decreasing area [9]. The maximum extrusion force was achieved at 1260 kN through experimentation. The extrusion force, die angle, land height 5 mm, were measured using both FEA and experimentally. These two results are compared and better results are reported, for two different methods have their merits and demerits. The FE model does not take into account changes in the frictional coefficient at the billet-die interface caused by lubricant breakdown or thermal softening of the billet. The largest inaccuracies were found at the smallest reduction ratios when extrusion force values acquired using the FE programme

***CORRESPONDING AUTHOR | K. A. Francy** | ✉ anupamafrancy.k@vishnu.edu.in
© The Authors 2023. Published by Universiti Malaysia Pahang Publishing. This is an open access article under the CC BY-NC 4.0 license

were compared to those obtained by computation. However, the FEA prediction error is less than 11% at larger reduction ratios, where the die exit diameter is 9 and 5 mm.

Adeosun et al. [10] carried out an experimental examination on the effects of the decrease in area, die angle, different loads on the various external pressures, and fluid flow method of the cold extrusion technique. The aluminium alloy used as flow fluid material and lead material used as inner circular section with four symmetrical views. It is observed that, a die angle of 90° resulted in the lowest extrusion force and non-dimensional specific coring pressure, which is suitable for die design to reduce extrusion pressure and to increase the die life.

Extrusion simulations were carried out by Zhou et al. [11, 12] using round and square dies for the material Aluminum 6061 alloy at the reduction ratios of 20:1 and 60:1. Rao et al. [13] use numerical analysis to determine the ideal process variables (die angle, ram speed coefficient of friction) for the extrusion of the aluminium 6061 alloy. Several experimental and numerical studies on the influence of the aforementioned factors during the extrusion process can be found in the literature [14, 15]. Cold forming techniques can produce hardness levels that are significant in percentage. The consequence of die angles 30°, 45° and 60° on surface finish hardness of cold forward extrusion for AA 6351 & AA 1100 was investigated experimentally. Experiments are conducted to calculate the lowest extrusion force and to identify effective die entrance angles for materials like aluminium, lead and steel [16]. The deformation behavior of the Aluminum 6063 alloy during the extrusion process are investigated by Gbenebor et al. [17]. The dies are made of tool steel and with die entrance angles of 15°, 30°, 45°, 60° and 75°. The deformation zone length is calculated with known die angle and extruded diameter. It is revealed that die angle 15° yields highest low flow stress encountered. The external parameters are strength, stress, strain and plastic deformation are attain better results at 75° die angle in Al-Mg-Si alloy. When the die angle is increased, the deformation zone length decreases and the axial deformation zone increases in comparison to the lateral deformation zone for a die angle of 45°, along with decreased ductility.

In addition to identifying the ideal process parameters, Hosseini et al. [18] investigated the impact of extrusion process parameters on the response of extrusion force. The dies with different die angles (5°, 7.5°, 10°, 12.5°and 15°) were considered to know the influence of die angle. From the results, it is concluded that input value of area reduction, 15° die angle is an optimal value than compared with other die angles. The hardness and surface roughness of a finished part has to be evaluated to ensure the quality of the product, strength, and formability. Measurements are drawn for two different metals through five different extrusion ratios with the help of Brinell hardness number in cold forward extrusion [19]. Higher surface roughness and lower hardness have been recorded among the products extruded with grease lubrication at 45° die angle. The extrusion pressure is decreased along the walls of the die with an increased ram speed for billets of Aluminium 6063 [20]. A fine structure with high integrity coarse grains is further achieved by increasing ram speed. The microstructure of AA 6063 has been studied to establish the relationship between the presence of Al, Fe, Si, and Mg_2Si phases and the quality of the extruded product. When the die entry angle is increased, the dislocation motion is clearly reduced in Al, Fe, and Si along with higher hardness [21]. A proportionate impact on the geometry and scattering of evident phases has been observed with an influence of die entrance angle on the flow material because of contact area between the die wall and work piece increased. A similar kind of behaviour is observed from researches Akbar and Yaseen [22]. Commercial and military aircraft, as well as Navy ships and aircraft (wing and fuselage) structures, frequently use the AA2024 material [23, 24]. Although, the deformation behavior (load-punch displacement curves) of AA 2024 alloy and significance of the process parameters in the cold forward rod extrusion tests have not yet addressed. A proportionate impact on the geometry and scattering of evident phases has been observed with an influence of die entrance angle on the flow material. Decreasing the die angle increases the homogeneity of deformation [25]. The force-displacement curve of extrusion, stress distribution and strain distribution are all examined to circular cups [26]. Higher friction & larger pressure values are required to perform the extrusion process by considering the paramters extrusio ratio and die profile [27]. The parameters such as number of passes and die angle that effect on Equal Channel Angular Extrusion process has analysed. Tensile strength and hardness of Aluminium 6063 treated by ECAE were examined using response surface methods [28]. Soft computing methods are one of the technique that can be utilised for prediction because the tests are carried out with varied combinations of process factors [29]. Artificial Neural Network modeling is used to forecast the dimensional accuracy of extruded products.

A conclusion drawn from the literature is that, the key process variables, such as die angle (DA), punch speed (PS), and lubricant, have a considerable impact on the extrusion output characteristics. The impact of these parameters on the extrusion process is therefore empirically investigated in the current work. Extrusion force, displacement, time, and surface roughness are to be considered as the output extrusion process parameters. Electron Back Scatter Diffraction (EBSD) technique is used in the present work to investigate the grain size, sub grain sizes and grain misorientation distrubution after the deformation process extrusion. AA 2024 alloy is chosen as work piece material for the experimentation.

2.0 METHODS AND MATERIALS

Table 1 lists the AA2024 material's chemical composition. The chemical composition of the AISI D2 steel used to make the die and punch is displayed in Table 2. The quality of the final extruded component depends on a few factors, including punch speed, die angle, work piece length & diameter, coefficient of friction, extrusion ratio, material flow, and die land height. Thus, fundamental factors like punch speed, die angle, and lubricants are selected in the current work.

The input process parameter levels are tabulated in Table 3. The other parameters like work piece diameter, length, and extrusion ratio are maintained as constant for all the experiments and the details are presented in Table 4.

Table 1. Element composition of AA 2024 [23]

Element	Fe	Zn	Cu	Si	Mg	Cr	Ti	Mn	Al
Composition (wt. %)	0.49	0.26	3.99	0.49	1.49	0.09	0.14	0.48	94.69

Table 2. Element composition of AISI D2 [30]

Element	C	Si	Cr	Mn	Mo	V
Composition (wt. %)	1.50	0.30	12.0	0.40	0.8	0.8

Table 3. Input parameters and their levels [31]

Process Parameters	Symbol	Level 1	Level 2	Level 3
Die Angle (deg)	DA	10	20	30
Punch Speed (mm/min)	PS	1.6	3.2	4.8
Lubricant	CoF	MoS_2	Zinc Stearate	Grease

Table 4. Geometrical details of die, work piece and punch tool

Parameter	Dimension
Work piece diameter	32mm
Extruded work piece diameter	28 mm
Work piece length	20 mm
Extrusion ratio	1.3
Top die height	60 mm
Top die inside diameter	32.1mm
Outside diameter of the topdie	96 mm

2.1 Experimental Procedure of Extrusion Process

The setup for the cold extrusion process has been created and equipped with a 100T hydraulic press depicts in Figure 1. A cylindrical bars of AA 2024 were extruded with the help of hydraulic press. The experiments were run on a computer-controlled hydraulic press at punch speeds of 1.6 mm/min, 3.2 mm/min and 4.8 mm/min. A load transducer attached to the punch monitored the extrusion force. a personal computer was used to manage the data acquisition system. A cylindrical billet of 32 mm diameter was positioned inside the container before the extrusion procedure then the punch upset the work piece. After the material had filled the die opening, it was extruded out of the die in a forward motion to create a rod/bar with the desired size. The work piece was ejected after the extrusion process was finished. The dies required frequent replacement. Dies were made of AISI D2 steel. Different die angles between 10° and 30° were used to measure the changes in extrusion force. Figure 2 depicts the extrusion process geometry of punch and die. Figure 3(a) and (b) illustrates the die and punch before assembly of the extrusion process. The work piece samples initially subjected to Annealing treatment consists of heating the billets to 345 °C in an muffel furnace then soaked in the furnace for an additional 15 minutes before being cooled to room temperature [14]. The purpose of heat treatment done on workpiece is to improve its mechanical attributes, such as strength, prevent wear, and reduce residual stresses.

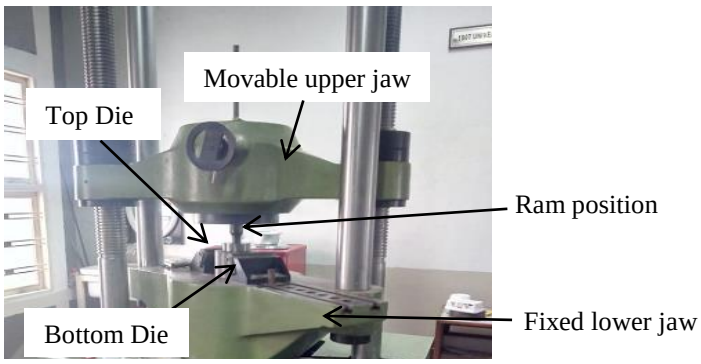

Figure 1. Experimental set up for extrusion process

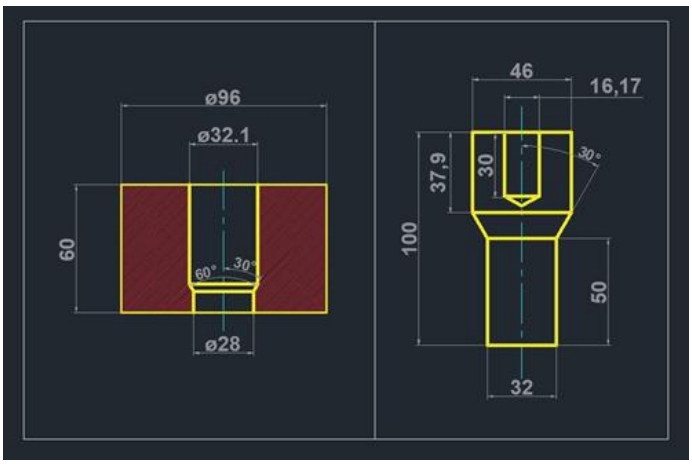

Figure 2. Schematic diagram of die and punch extrusion process for 30° die angle

(a) (b)

Figure 3. Individual parts before the extrusion process: (a) dies and (b) punch

2.2 Surface Roughness of the Work Piece Surface

The surface roughness was measured on the surface of work piece samples after extrusion process were performed. Industries measures surface roughness to understand how a real object interacts with its surroundings. Decreasing the surface roughness usually increases its manufacturing costs. The measurement of the values R_a is performed using Mitutoyo surf test SJ301 equipment with high accuracy (resolution of 0.002 µm at a measurement range of 25 µm). To determine the surface roughness value, the average of five locations were taken into consideration.

2.3 Microstructural Investigation

For microstructure investigations, extruded work pieces were polished and chemically etched using Keller's reagent. Under 150X magnification, the samples microstructure is inspected using a stereo microscope.

2.4 Electron Backscatter Diffraction Analysis Method

The Electron Backscatter Diffraction (EBSD) acquisition was performed in a Sigma Field Emission Scanning Electron Microscope equipped with a Nordif Ultra-Fast detector and software (see Figure 4). The procedure which was used to determine the sub grain size and the misorientation is embedded in the EBSD software. At first the particles size is measured. The program needs to be set with minimum step size to obtain 111 good resolutions on the actual picture. To achieve good resolution, it is necessary to have a minimum of 10 pixels within a small grain. Then the measurements are started which are based upon pixel numbers in each grain. These measurements are used in the calculations where grains and sub grains are identified based upon grain boundaries. Each pixel has a diffraction pattern which is used in the calculations. Sub grains are defined with low angle boundaries <15º.

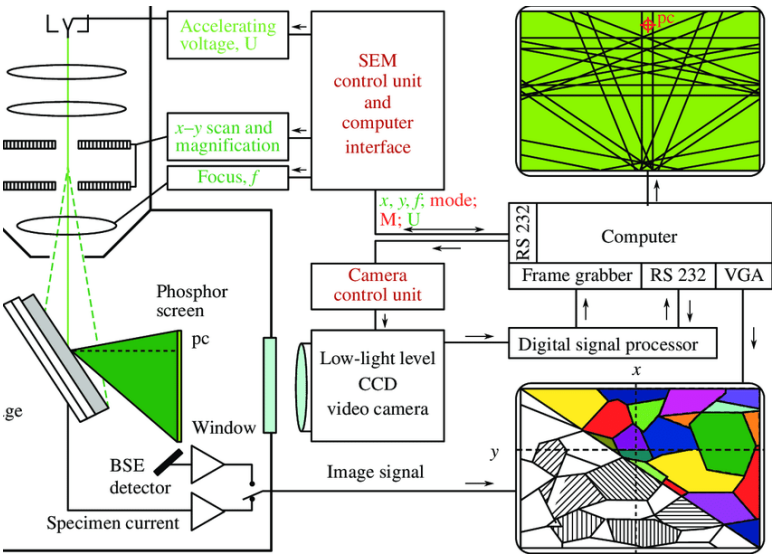

Figure 4. Schematic diagram of EBSD setup

The sub grain size measurements and misorientation analysis were performed by means of EBSD analysis (Electron Backscatter Diffraction) method. The samples were ground at 220, 320, 500 and 1200 mesh and polished with 3µm and 1µm diamond polish. After polishing, the samples were electro-polished in A2 electrolyte at 30V, flow rate 7 for 3-4 sec using a Struers LectroPol5. Samples are collected from representative areas within the sample and detailed samples for sub grain size and misorientation 1 mm² areas, in the edge zone of the samples are analyzed in the circular profiles. The locations of the sample area are chosen to be representative with respect to the structure visible in the micrographs depicts in Figure 5.

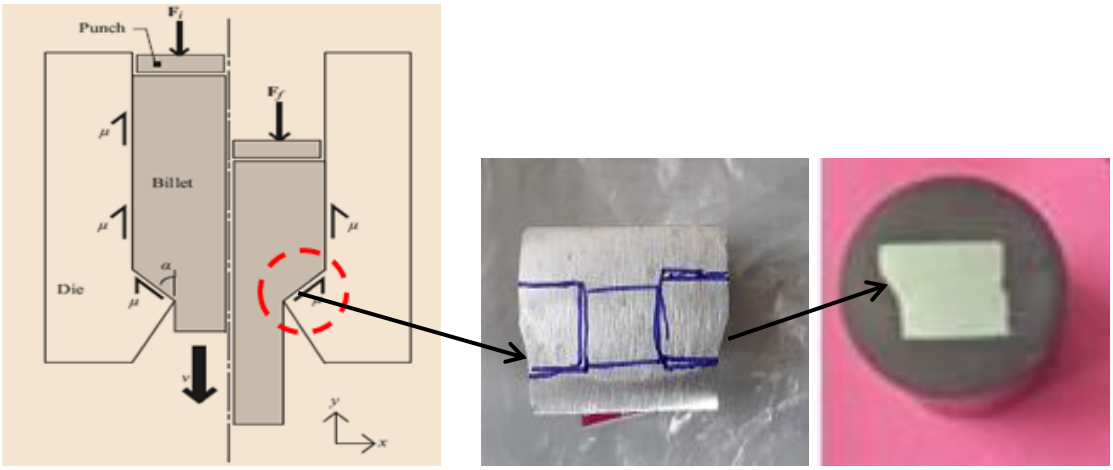

Figure 5. Deformed shape of the extruded work piece

3.0 RESULTS AND DISCUSSION

The cylindrical bars were extruded successfully with the help of hydraulic press with varying parameters of die angle, punch speed and lubricant. Experiments are conducted according to L_{27} orthogonal array and responses are presented in Table 5.

Table 5. Response table of extrusion parameters

Exp. no	Die Angle (deg)	Punch Speed (mm/min)	Lubricant	Displacement (mm)	Time (min)	Extrusion Force (kN)	Surface roughness (µm)
1	10	1.6	MoS_2	12.95	16.06	132.25	2.96
2	10	1.6	phosphate sulphur	13.06	12.60	137.80	1.87
3	10	1.6	grease	13.68	10.21	138.04	1.14
4	10	3.2	MoS_2	14.04	13.58	158.24	2.47
5	10	3.2	phosphate sulphur	14.53	10.35	159.02	1.85

Table 5. (cont.)

Exp. no	Die Angle (deg)	Punch Speed (mm/min)	Lubricant	Displacement (mm)	Time (min)	Extrusion Force (kN)	Surface roughness (μm)
6	10	3.2	grease	14.96	7.33	162.06	1.24
7	10	4.8	MoS_2	15.02	10.50	171.28	2.01
8	10	4.8	phosphate sulphur	15.53	8.71	173.88	1.70
9	10	4.8	grease	16.07	5.67	176.00	1.11
10	20	1.6	MoS_2	16.76	15.19	179.12	1.76
11	20	1.6	phosphate sulphur	17.04	8.94	182.76	0.88
12	20	1.6	grease	17.67	6.79	186.94	0.59
13	20	3.2	MoS_2	18.02	13.19	184.32	1.72
14	20	3.2	phosphate sulphur	18.64	8.04	189.88	1.06
15	20	3.2	grease	18.89	5.79	194.67	0.66
16	20	4.8	MoS_2	18.95	11.32	224.10	1.48
17	20	4.8	phosphate sulphur	18.99	7.94	236.01	1.02
18	20	4.8	grease	19.09	4.79	260.01	0.43
19	30	1.6	MoS_2	19.62	14.72	286.01	1.24
20	30	1.6	phosphate sulphur	20.12	8.81	298.38	0.33
21	30	1.6	grease	20.95	4.92	310.34	0.19
22	30	3.2	MoS_2	21.96	14.12	313.24	1.02
23	30	3.2	phosphate sulphur	22.55	7.57	314.95	0.50
24	30	3.2	grease	23.68	4.04	316.05	0.16
25	30	4.8	MoS_2	24.07	13.01	319.66	0.87
26	30	4.8	phosphate sulphur	24.64	6.98	326.36	0.51
27	30	4.8	grease	25.87	3.92	333.66	0.12

3.1 Extrusion Force on the Flow Stress

The minimum extrusion force , displacement , time , and compressive strength are recorded to know the influence of the DA, PS and lubricant. Figures 6(a), (b) and (c) show the workpieces after the extrusion process at 10° and 20° die angles at a punch speed of 3.2 mm/min. It has been found that, with 10° die angle, punch speed (1.6 mm/min) and lubricant (MoS_2) results in a minimum extrusion force of 132.25kN, displacement of 12.95 mm and compressive strength of 182.282 MPa.

Figure 6. Samples after the extrusion at: (a) 10°, (b) 20° and (c) 30° die angles

The impact of die angle on the extrusion output responses is shown in Figures7 (a) to (d). For the fixed die angle, the mean of the output responses (varying the punch speed and lubricant) is considered and is shown in Figure 7. As the die angle increases, the extrusion force and displacement enhances (see Figures 7(a) and (b)), whereas the surface finish and time to complete the extrusion process is decreases (see Figures 7(c) and (d)). The rate of enhancement in the extrusion force with an increase of die angle ranges from 10° to 20° is as low as compared with an increase of die angle 20° to 30°. It is noticed that 26% and 32.53% increase of extrusion force takes place if the die angle changes 10° to 20° and 20° to 30°. A similar kind of behavior is observed from earlier researches Akbar and Yaseen [22]. The increased contact area between the die wall and billet causes the displacement to increase as indicated in Figure 7(b), and the time taken for the complete extrusion process decreases (see Figure 7(c)). The surface roughness value is decreased with an increase of lubrication as shown in Figure 7(d).

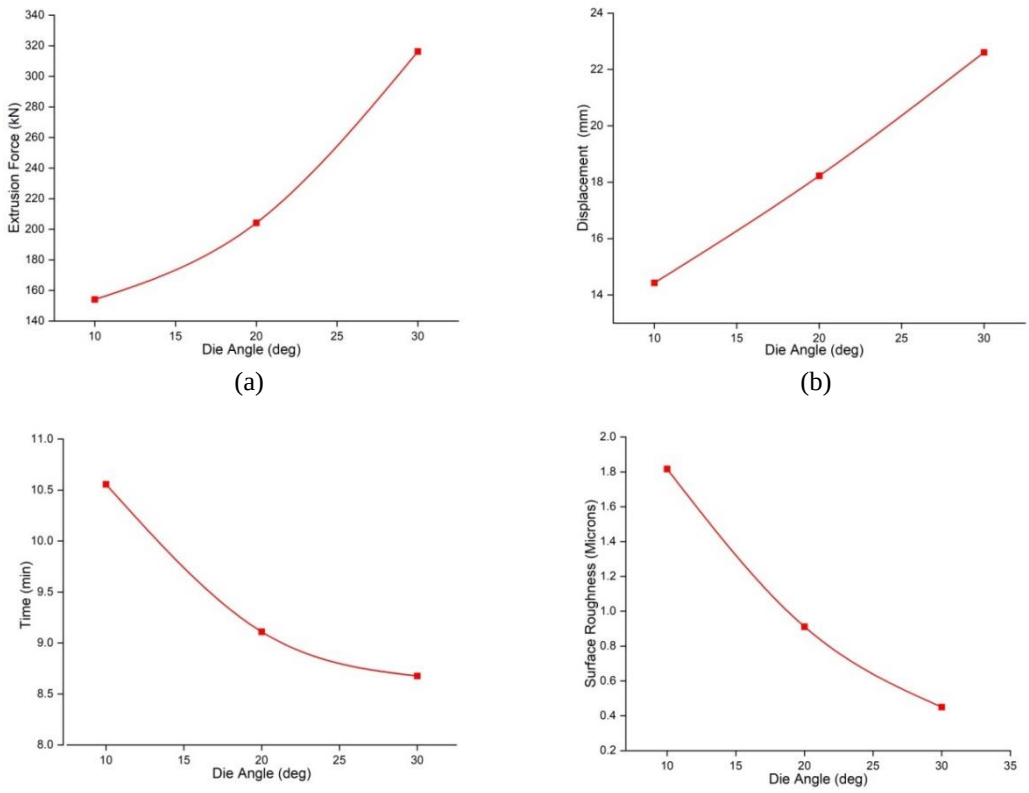

Figure 7. Effect of die angle on: (a) extrusion force, (b) displacement, (c) time and (d) surface roughness

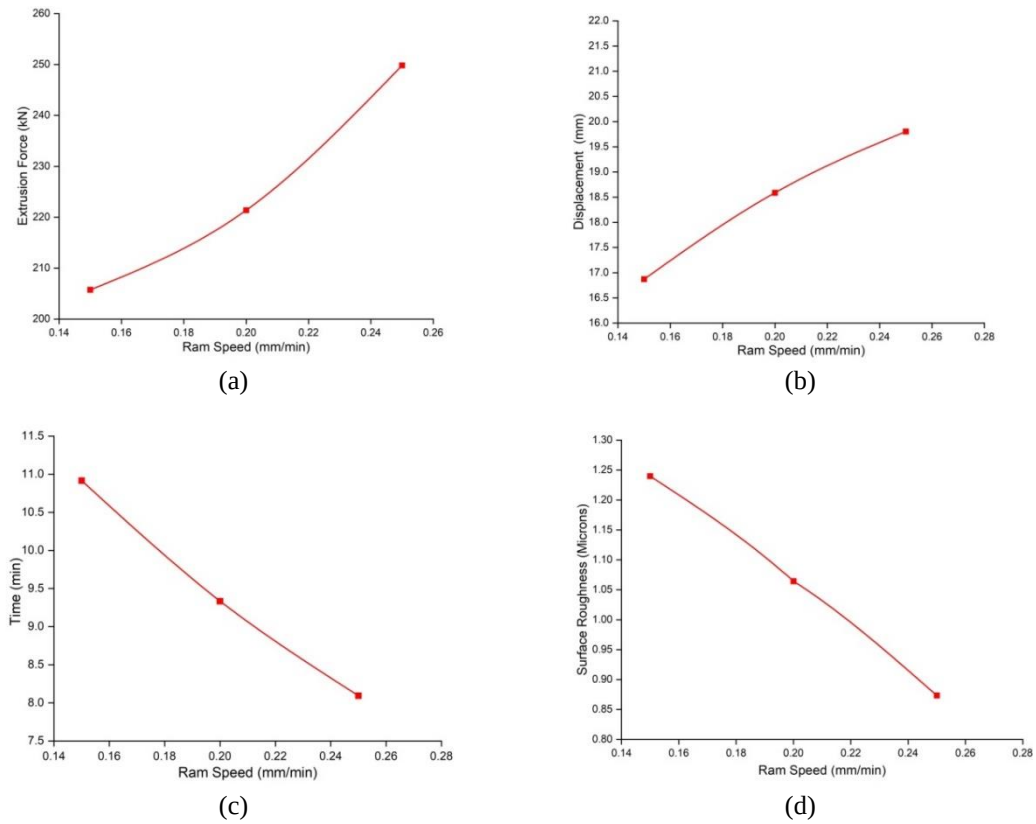

Figure 8. Effect of punch speed on: (a) extrusion force, (b) displacement, (c) time and (d) surface roughness

The impact of punch speed on the extrusion output responses is shown in Figure 8. The mean of the output responses (varying the die angle and lubricant) is considered and is presented in this figure. Similar to the die angle, punch speed have a similar influence on the extrusion output responses. However, the behaviour trend is not similar for the

displacement, extrusion force, and surface roughness. With an enhancement of punch speed, the displacement is increased, as compared with die angle the displacement variation is less. The extrusion force and time to complete the extrusion process are linearly varies with punch speed, the rate of enhancement/decrement for these responses is lower as compared with die angle variation.

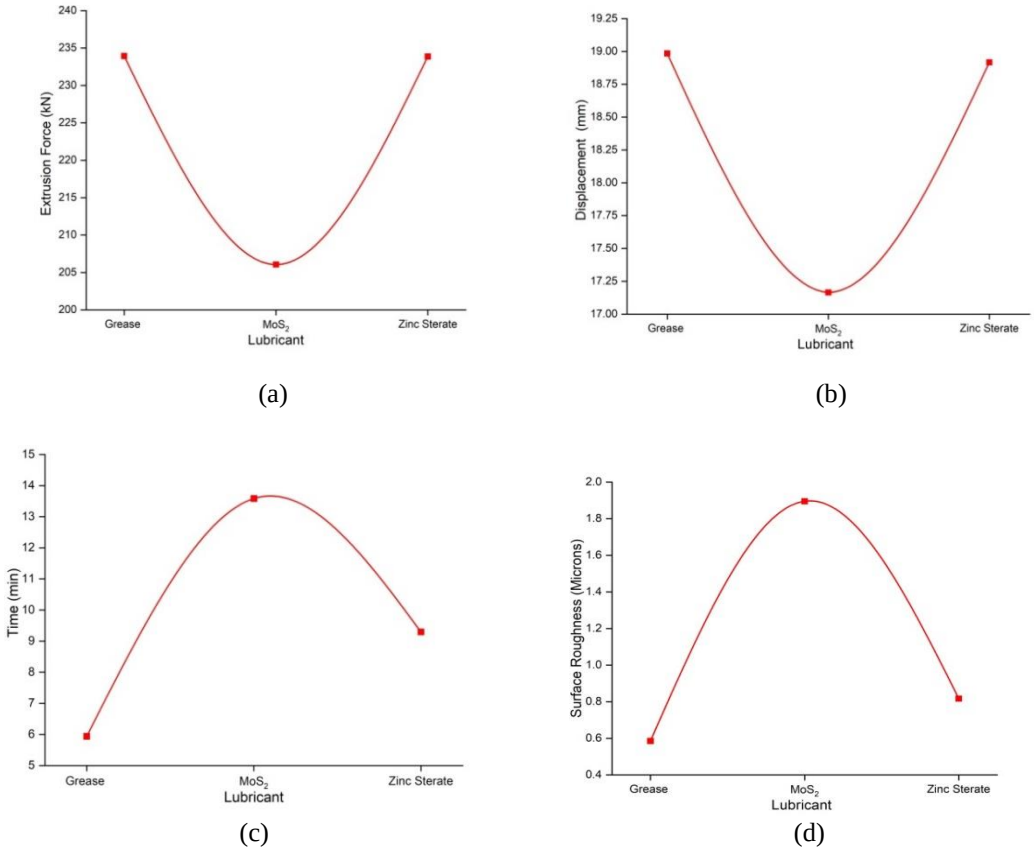

Figure 9. Effect of lubricant on: (a) displacement, (b) extrusion force, (c) time and (d) surface roughness

Similar to this, Figure 9 depicts the influence of lubricant on extrusion output responses. Here, the mean of output responses (by varying the die angle and punch speed) is considered. Peculiar behaviour has been observed in the output responses with different lubricants. It is noticed that the use of grease or zinc stearate as lubricant in the extrusion process favorable results are obtained. While using MoS_2 as a lubricant in the extrusion process, high surface roughness values are obtained. During the extrusion process, it is also observed that, MoS_2 quickly evaporates; with this, the low quality of the product is obtained [17].

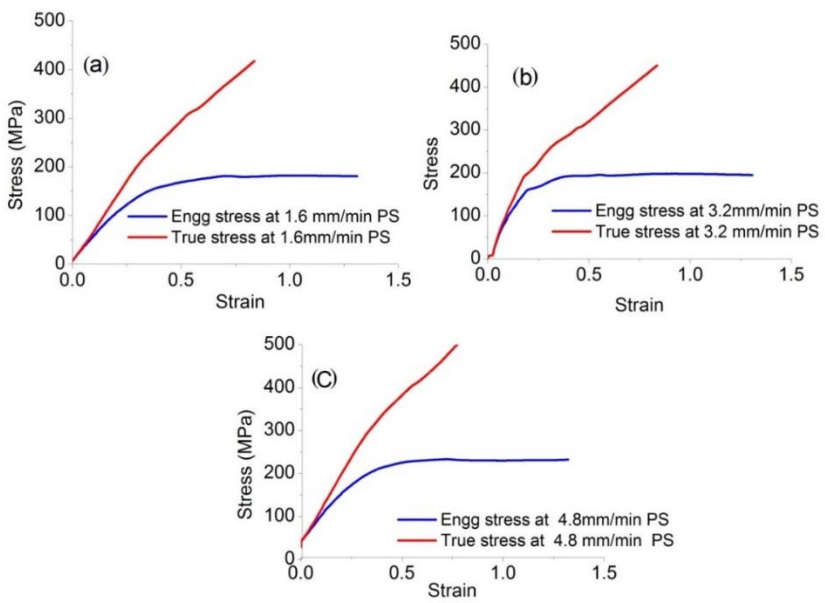

Figure 10. The stress-strain diagram at 10° die angle for punch speeds: (a) 1.6 mm/min, (b) 3.2 mm/min and (c) 4.8 mm/mi

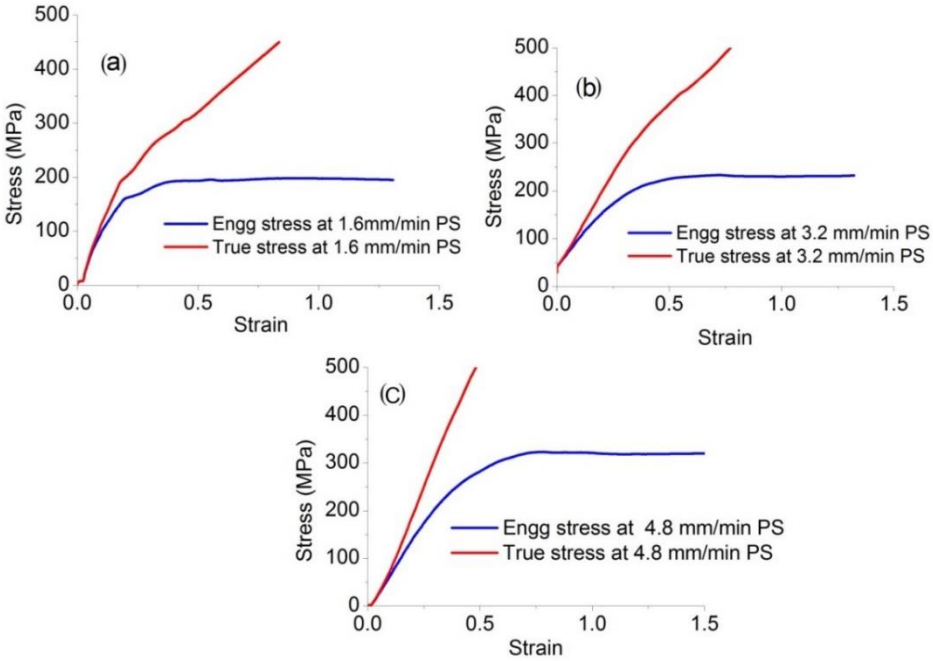

Figure 11. The stress-strain diagram at 20° die angle for punch speeds: (a) 1.6 mm/min, (b) 3.2 mm/min and (c) 4.8 mm/min

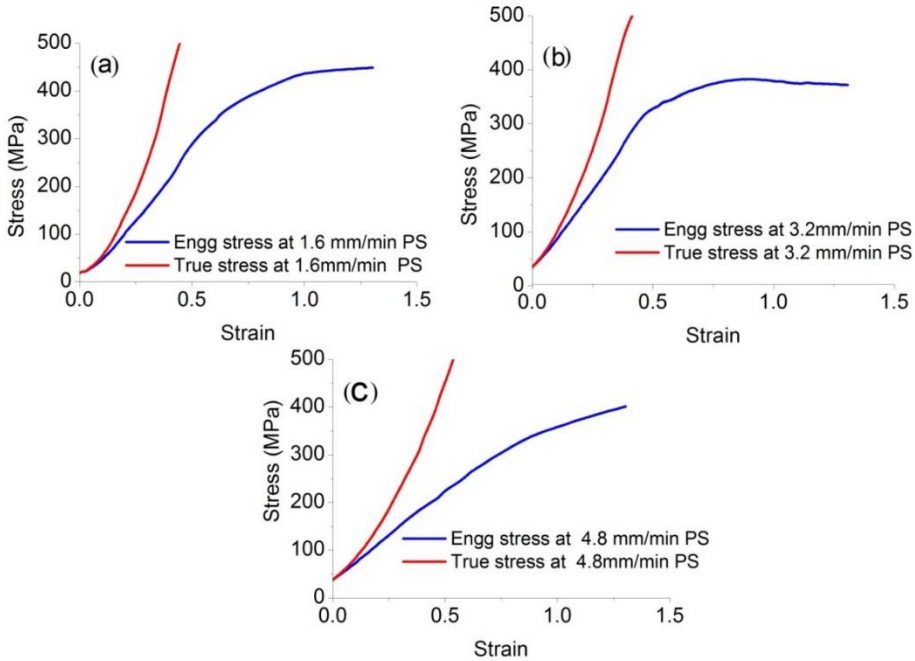

Figure 12. The stress-strain diagram at 30° die angle for punch speeds: (a) 1.6 mm/min, (b) 3.2 mm/min, and (c) 4.8 mm/min

Figure 10 to 12 show the flow curves for true stress-strain and engineering stress-strain for die angles of 10°, 20° and 30°, respectively, at different punch speeds (1.6 mm/min, 3.2 mm/min, and 4.8 mm/min). From the curves, it is observed that the stress increases with increasing of strain. Higher tensile strength in the material will decrease the extent of cold extrusion deformation but may make the material more brittle in nature.

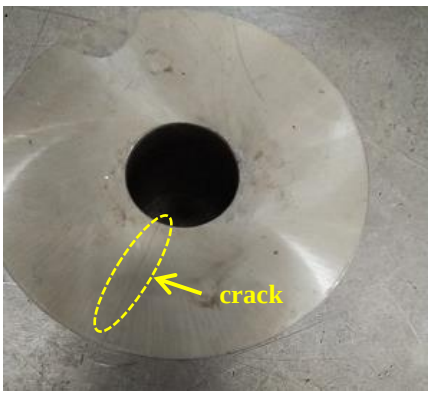

Figure 13. Punch speed of 4.8 mm/min causes crack to 30° DA

The impact of the lubricant on the extrusion force is minimal, but it has a substantial impact on the crack. The experiments conducted by using grease and fixing the punch speed and varying the die angle, its influence on extrusion force and surface roughness is significant. By fixing the die angle and increasing the punch speed extrusion force increases and damage behavior is peculiar. The great amount of extrusion force may lead to a crack formation on the circumference of the extruded product. A crack was initiated around the billet at 4.8 mm/min punch speed for 30° die angle and the crack is not occurred at punch speed less than 4.8 mm/min to the same die angle. Besides, if the punch speed enhances on or above 4.8 mm/min more crack was observed. Hence the die is also subjected to crack as seen in Figure 13 [32].

3.2 Microstructure Examination

The optical micrograph of Al-Cu alloy before extrusion is shown in Figure 14(a), which reveals the presence of equiaxed grain with an average grain size of 200±20μm in the x-direction and 100±25μm in the y-direction. Figure 14 (b) – (d) depicts the micrograph of components at die angles 10°, 20° and 30°. In the deformation zone at 10° die angle, very few deformed grains are visible with the structure of small elongated grains. The grains allow very smooth and easy flow at 20°die angle when compared to 10° die angle. Fine elongated grains are developed in the extrude at 20° DA (see Figure 14(c)). The extruded sample at 30° die angle exhibits a severe deformation of grains. With an increase in die angle from 10° to 30°, grain refinement can be observed and the microstructure revealed diffused and ill-defined grain boundaries. This is attributed to the severe strain induced both within the grains and at grain boundaries and also to the high stacking fault energy of Aluminium alloys.

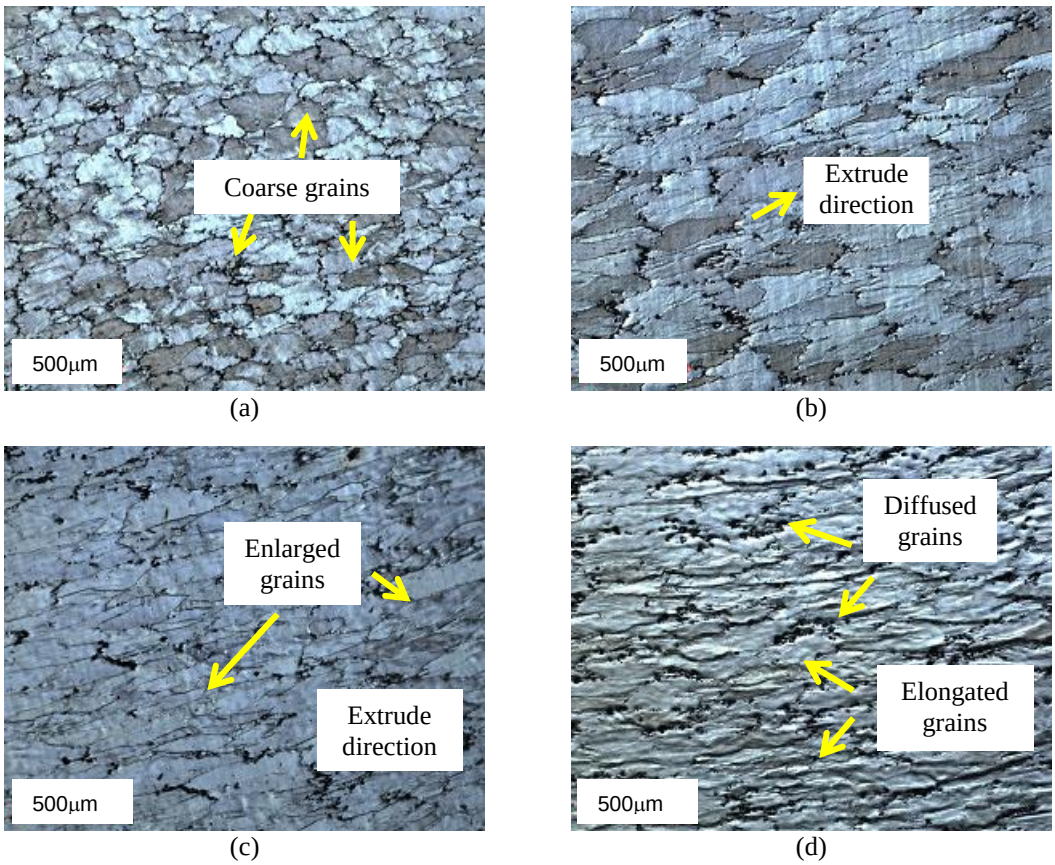

Figure 14. Micrographs of AA 2024 alloy samples: (a) before extrusion, (b) 10° DA, (c) 20° DA and (d) 30° DA

3.3 Deformation during Extrusion Process

To evaluate the real grain morphology at the various die angles employed in the experiments, EBSD techniques are to further investigate the structure of the extruded work piece. The original grain structure are deformed during extrusion process, resulting in a recrystallized structure after the extrusion process. A thick black line on the EBSD map indicates a grain boundary and representing a misorientation between grains. When the misorientation between grains and sub grains is less than 6°, sub grains are usually described. The majority of angles of misorientation across the boundaries are smaller than 25°. After extruding the work piece at 30° die angle, the microstructure showed grain refinement.

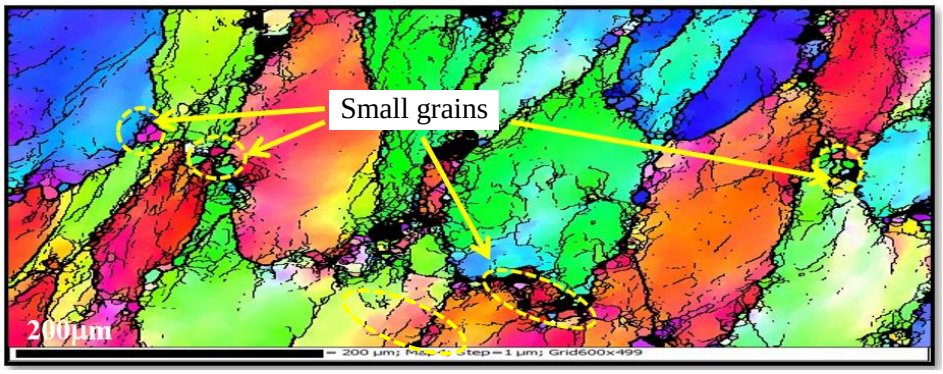

Figure 15. EBSD graphs from the corner zone of extruded work extrusion at 20° die angle for 4.8 mm/min ram speed

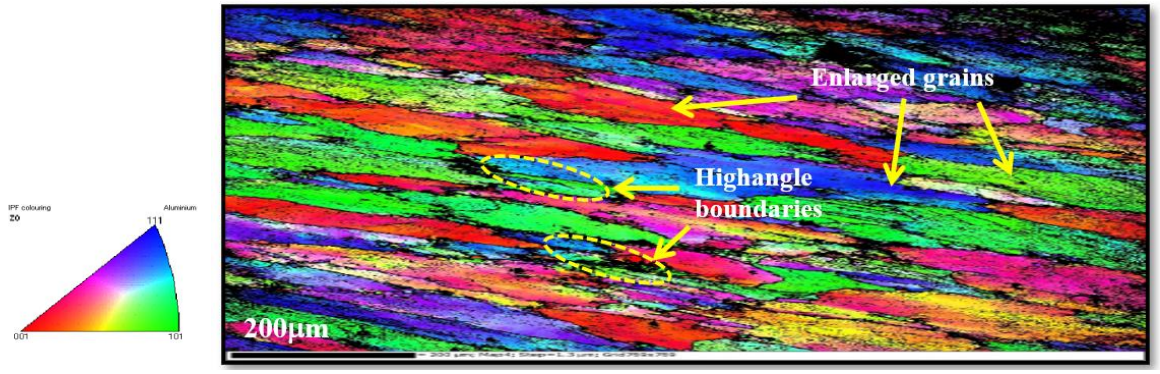

Figure 16. EBSD graphs from the corner zone of extruded work extrusion at 30° die angle for 4.8mm/min ram speed

Figure 15 and 16 show the EBSD graphs of the work piece sample after the extrusion process at 20° die angle and 30° die angle with a ram speed of 4.8mm/min. It shows large number of fractions for misorientation in the < 6° range. A misorientation angle of < 6° is found in approximately 49 % of the sub grains is observed. The distribution data showed a peak at 2° which matched to the microstructure's predominance of sub grains during the extrusion process. The majority of grains are oriented in the direction of {101}.

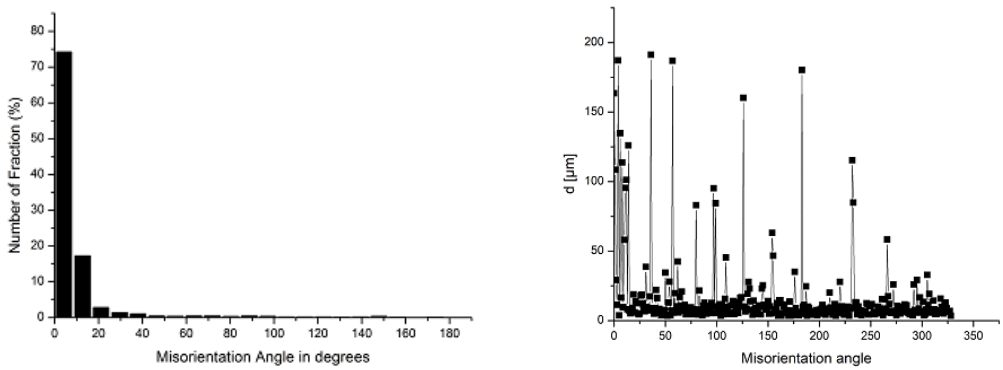

(a) (b)

Figure 17. (a) Misorientation and (b) distribution of misorientation between the grains obtained by EBSD at 30° die angle (4.8mm/min)

Figure 17 depicts graphical representation of misorientation measurement for a sample at 30° die angle. The graphs shows, work piece samples extruded at 30° die angle with a punch speed of 4.8 mm/min have great high angle boundaries

with misorientation angle above 40° degrees. The average grains for all examined grains inside the specified area are calculated using the EBSD software. After the extrusion process, a bimodal distribution pattern is produced as a result of the distribution of misorientation shifting toward higher angles as the strain increases. During the extrusion process, the grains aspect ratio is gradually reduced. As a result, a microstructure with distinct features such as nearly equiaxed grains and a large number of high-angle boundaries evolves uniform microstructure.

4.0 CONCLUSIONS

The present work emphasized the influence of the process parameters on the cold extrusion process studied experimentally. Extrusion force, displacement, time and surface roughness are taken into account as responses while using the AA 2024 alloy as the work piece material.

1) The extrusion force has been increased with an increased die angle range from 10° to 30°. During the deformation process, material flow is influenced by die angle and punch speed. The quality of the final product and extrusion force is impacted by material flow.
2) Due to the dead metal zone, it becomes more challenging to extrude the material at 10° die angle. The displacement of the work piece decreases, and the extruded time increases while extruding the material at10° die angle.
3) A crack is observed with 30° die angle at a punch speed of 4.8 mm/min. Hence, punch speed higher than 4.8 mm/min is not recommended for 30° die angle. The damage occurred on the surface of the billet after certain displacement from the die exit. The damage is considerable at 30° die angle under the punch speed of 4.8mm/min.
4) At 30° die angle, the extrusion performance characteristics are good and fine column grains have been observed in the microstructure.
5) High angle boundaries with misorientation above 40° degrees are present when extrusion punch speed is increased at a 30° die angle.

5.0 REFERENCES

[1] L. Deng, J. Xia, and X. Wang, "Precision forging presses for aluminum alloy," *Frontiers of Mechanical Engineering*, vol. 13, no. 1, pp. 25–36, 2018.

[2] Aluminum Extruders Council, "Aluminum Extrusion Manual," *4th ed., Aluminum Extruders Council,* Wauconda, Illinois, USA, 2014.

[3] S. Murtaza Ali, "To study the influence of frictional conditions and die land length on component error and die deflection in cold extrusion by finite element analysis," *Journal of Metallurgical Engineering*, vol. 2, no. 1, pp. 29–38, 2013.

[4] S. O. Adeosun, E. I. Akpan, and O. P. Gbenebor, "Extrusion characteristics dependence of wrought aluminium alloy on extrusion variables," *American Journal of Material Science*, vol. 3, no. 4, pp. 77–83, 2013. 03.

[5] A. F. M. Arif, A. K. Sheikh, and S. Z. Qamar, "A study of die failure mechanisms in aluminum extrusion," *Journal Material Processing Technology*, vol. 134, no. 3, pp. 318–328, 2003.

[6] L. Chen, G. Zhao, J. Yu, W. Zhang, and T. Wu, "Analysis and porthole die design for a multi-hole extrusion process of a hollow, thin-walled aluminum profile," *International Journal of Advanced. Manufacturing Technology*, vol. 74, no. 1–4, pp. 383–392, 2014.

[7] N. Carvalho, A. Correia, and F. de Almeida, "The evaluation of defects in the aluminium extrusion process through quality tools," *WSEAS Transactions on Environment and Development*, vol. 14, pp. 1–15, 2018.

[8] S. O. Onuh, M. Ekoja, and M. B. Adeyemi, "Effects of die geometry and extrusion speed on the cold extrusion of aluminium and lead alloys," *Journal of Material Processing Technology*, vol. 132, no. 3, pp. 274–285, 2003.

[9] P. Tiernan, M. T. Hillery, B. Draganescu, and M. Gheorghe, "Modelling of cold extrusion with experimental verification," *Journal of Material Processing Technology*, vol. 168, no. 2, pp. 360–366, 2005.

[10] S. O. Adeosun, O. I. Sekunow, and O. P. Gbenebor, "Effect of die entry angle on extrusion responses of aluminum 6063 alloy," *International of Engineering and Technology*, vol. 4, no. 2, pp. 127–134, 2014.

[11] J. Zhou, L. Li, and J. Duszczyk, "3D FEM simulation of the whole cycle of aluminium extrusion throughout the transient state and the steady state using the updated Lagrangian approach," *Journal of Material Processing Technology*, vol. 134, no. 3, pp. 383–397, 2003.

[12] T. Chanda, J. Zhou, and J. Duszczyk, "FEM analysis of aluminium extrusion through square and round dies," *Materials and Design*, vol. 21, no. 4, pp. 323–335, 2000.

[13] T. B. Rao and A. G. Krishna, "Design and optimization of extrusion process using FEA and taguchi method," *International Journal of Engineering Research and Technology*, vol. 1, no. 8, pp. 1–5, 2012.

[14] G. A. Chaudhari, S. R. Andhale, and N. G. Patil, "Experimental evaluation of effect of die angle on hardness and surface finish of cold forward extrusion of aluminum," *International Journal of Emerging Technology and Advanced Engineering*, vol. 2, no. 7, pp. 2–6, 2012.

[15] D. Rath and S. Tripathy, "Investigation of extrusion of lead experimentally from round section through equilateral triangular section converging dies at different area reductions during forward metal extrusion process," *International Journal of Engineering and Science*, vol. 3, no. 1, pp. 32–38, 2013.

[16] L. Gusel and R. Rudolf, "Different techniques for strain analisys in metal forming processes," in *Proceedings of the International Conference of DAAAM Baltic*, 2008, pp. 1–5.

[17] O. P. Gbenebor, O. S. I. Fayomi, A. P. I. Popoola, A. O. Inegbenebor, and F. Oyawale, "Extrusion die geometry effects on the energy absorbing properties and deformation response of 6063-type Al-Mg-Si aluminum alloy," *Results in Physics*, vol. 3, pp. 1–6, 2013.

[18] A. Hosseini, K. Farhangdoost, and M. Manoochehri, "Modelling of extrusion process and application of Taguchi method and ANOVA analysis for optimization the parameters," *Mechanika*, vol. 18, no. 3, pp. 301–305, 2012.

[19] A. Demir and F. O. Sonmez, "Prediction of brinell hardness distribution in cold formed parts," *Journal of Engineering Materials and Technology*, vol. 126, no. 4, pp. 398–405, 2004.

[20] A. F. M. Arif, A. K. Sheikh, S. Z. Qamar, and K. M. Al-Fuhaid, "Variation of pressure with ram speed and die profile in hot extrusion of aluminum-6063," *Materials and Manufacturing Processes*, vol. 16, no. 5, pp. 701–716, 2001.

[21] A. L. Rivas, P. Munoz, S. Camero, and O. Quintero-sayago, "Effect of the microstructure on the mechanical properties and surface finish of an extruded Al-6063 aluminum alloy," *Advances in Materials Science and Technology*, vol. 2, no. 1, pp. 15–23, 1999.

[22] A. A. Akbar, and R. S. Yaseen, "Study of the direct extrusion behavior of aluminum and aluminum alloy-2014 using conical dies," *Engineering & Technology Journal*, vol. 30, no. 6, pp. 950–958, 2014.

[23] Z. Liu, P. H. Chong, A. N. Butt, P. Skeldon, and G. E. Thompson, "Corrosion mechanism of laser-melted AA 2014 and AA 2024 alloys," *Applied Surface Science*, vol. 247, no. 1–4, pp. 294–299, 2005.

[24] T. Sheppard, "Extrusion of AA 2024 alloy," *Material Science and Technology*, vol. 9, no. 5, pp. 430–440, 1993.

[25] K. Murugesan, "Optimization of extrusion pressure using genetic algorithm," *International Journal of Innovations in Management, Engineering and Science*, vol. 6, no. 1, pp. 17–25, 2020.

[26] T. C. Chen, S. X. Chen, and C. C. Wang, "Punch motion curve in the extrusion–drawing process to obtain circular cups," *Machines*, vol. 10, no. 8, pp. 1–17, 2022.

[27] S. Z. Qamar, J. C. Chekotu, and S. B. Qamar, "Effect of shape complexity on ram pressure and metal flow in aluminum extrusion," *Journal of Materials, Minerals and Materials society*, vol. 71, no. 12, pp. 4378–4392, 2019.

[28] T. M. Azeez, L. O. Mudashiru, T. B. Asafa, O. M. Ikumapayi, A. S. Yusuff, and E. T. Akinlabi, "Effects of temperature, die angle and number of passes on the extrusion of 6063 aluminium alloy: Experimental and numerical study," *International Journal on Interactive Design and. Manufacturing*, pp. 1-11, 2022.

[29] A. K. Gupta and M. Taufik, "Investigation of dimensional accuracy of material extrusion build parts using mathematical modelling and artificial neural network," *International Journal on Interactive Design and Manufacturing*, vol. 17, no. 2, pp. 869–885, 2023.

[30] L. Bourithis, G. D. Papadimitriou, and J. Sideris, "Comparison of wear properties of tool steels AISI D2 and O1 with the same hardness," *Tribology International*, vol. 39, no. 6, pp. 479–489, 2006.

[31] A. F. Kothasiri, S. R. Chalamalasetti, and G. Peteti, "Multiple process parameter optimization of forward extrusion process on aa 2024," *International Jornal of Modern Manufacturing Technology*, vol. 13, no. 2, pp. 63–75, 2021.

[32] D. C. Chen, S. K. Syu, C. H. Wu, and S. K. Lin, "Investigation into cold extrusion of aluminum billets using three-dimensional finite element method," *Journal of Material Processing Technology*, vol. 192–193, pp. 188–193, 2007.